Performance Assessment of PV/T Air Collector by Using CFD

Wang, Z.
Department of Built Environment, University of Nottingham
(email: laxzw4@nottingham.ac.uk)

Abstract

Photovoltaic-thermal (PV/T) air collector, as a device by converting solar energy to electricity and thermal energy at the same time, was assessed by setting up models in the CFD program in this paper. A typical PV/T air collector was composed of glazing covers, PV panel, thermal collector, rear insulation and frame box. Seven models were named and developed after three different aspects, i.e., with or without glazing covers, semi-transparent or opaque PV panels, and air flow directions. Solar radiation on PV panel and thermal collector were pre-calculated and the results were used to input into the CFD program for further simulation. The simulation results were discussed. In general, the air flows in the air passages where its velocity and static temperature increased, however, the static pressure decreased. Maintaining other two variables, the study showed that the unglazed PV/T models would generate more electricity, but less thermal energy than the glazed PV/T models. As to the different transparency of PV panels, the semi-transparent PV panel models would generate more electricity, but less thermal energy than the opaque PV panel models. In terms of the air flow directions, both electricity and thermal energy were highly produced by straight air flow models.

Keywords: photovoltaic, thermal, CFD, electricity, heat

1. Introduction

Solar energy is the most important sustainable energy, which has the potential to meet the whole world's energy needs. The conversion of solar energy to electrical energy and thermal energy has been practiced for many years. By now, the widely used systems are photovoltaic (PV) system and thermal collector (T) system for the electrical and thermal generations, respectively. However, the waste heat from PV panel, high price of both two conventional systems and limited installation space on rooftop of the domestic houses prevent both systems being used simultaneously. An effective combination of both two systems is the photovoltaic-thermal (PV/T) collector system, producing heat and electricity at the same time, which is an advanced technology for the solar energy application. This kind of PV/T collectors has many advantages, i.e., competitive cost, more energy production, better building appearance. (Charalambous et al, 2007)

According to the different phase of the working fluid, PV/T collectors can be divided into PV/T liquid collectors and PV/T air collectors. Due to the minimal use of construction material and low operating costs, PV/T air collectors are utilized in many practical applications compared with the PV/T liquid collectors. Until now, many theoretical research and field experiments relating to the performance of PV/T air collectors has been conducted by various authors and has been published in various technical journals.

The aim of this paper is to investigate the performance of seven PV/T air collectors, which were named after with or without glazing cover, the transparency of PV panel (semi-transparent or opaque), and air flow direction (straight or U-shape). Based on flat-plate thermal collectors and photovoltaic panels, these systems were modelled and analyzed by using Computational Fluid Dynamics (CFD) simulation tool. The variation of air flow velocity, static temperature and static pressure were illustrated and the production of electricity and thermal energy were indicated from the simulation results.

2. Description of seven PV/T air collectors

The typical flat-plate PV/T air collectors, constituting of the glazing cover, PV panel, thermal collector, rear insulations and frame materials, are mounted on the rooftop or façades of a building. In general, solar radiation striking on the surface of PV panel, which is upon the thermal collector, is absorbed after transmitting through the glazing cover. Part of the solar radiation will be converted into electricity by PV panel, which, however, will generate heat as a result of its increased temperature. The air passing through the above and under air passages of thermal collector can eliminate the heat. The function of the thermal collector is to cool the PV panel down for more electricity generation and at the mean time produce more thermal energy. The glazing cover, above the PV panel, is to maximize the absorption of solar energy while minimize heat losses from inside to ambient. A metal frame surrounding the system and the rear insulation materials are used to reduce energy losses as well. (Modest, 1993)

The schematic of the proposed seven collectors were shown in Figure 1, which could be named as follows:

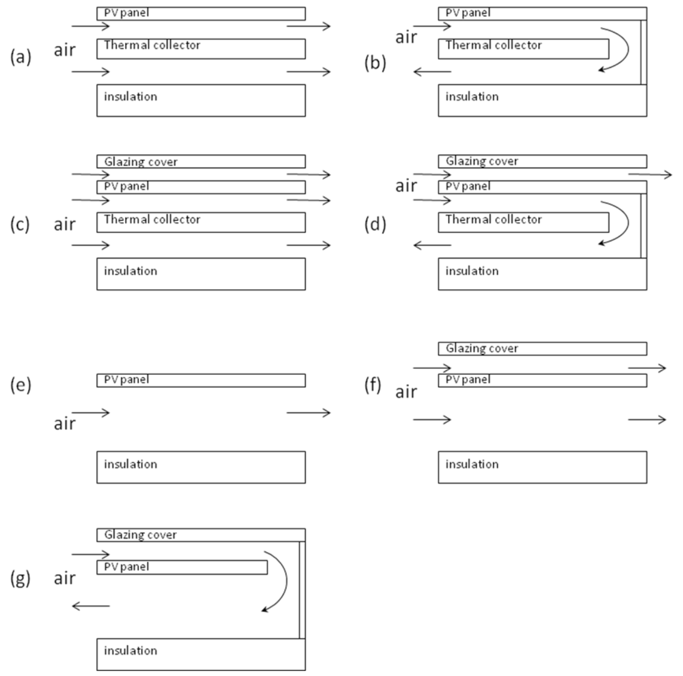

(a) Unglazed, semi-transparent PV panel, straight airflow collector
(b) Unglazed, semi-transparent PV panel, U-shape airflow collector
(c) Glazed, semi-transparent PV panel, straight airflow collector
(d) Glazed, semi-transparent PV panel, U-shape airflow collector
(e) Unglazed, opaque PV panel, straight airflow collector
(f) Glazed, opaque PV panel, straight airflow collector
(g) Glazed, opaque PV panel, U-shape airflow collector

Figure 1: Schematic of seven PV/T air collectors

Taking a complicated (d) model as an example to illustrate the structure/configuration of this system, the components of the model and the overall size were shown in Figure 2, the assumption of weather conditions and the geometrical parameters of the components were shown in Figure 3.

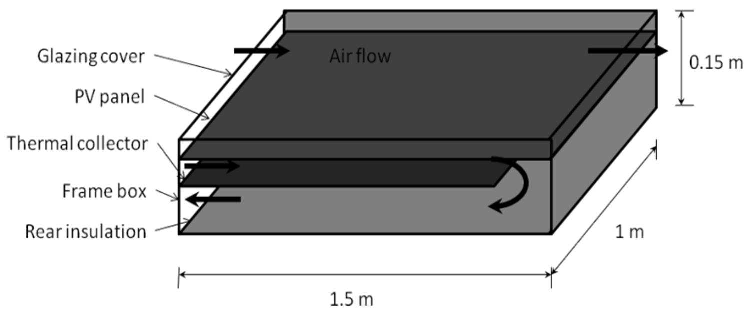

Figure 2: (d) model: system structure and overall size

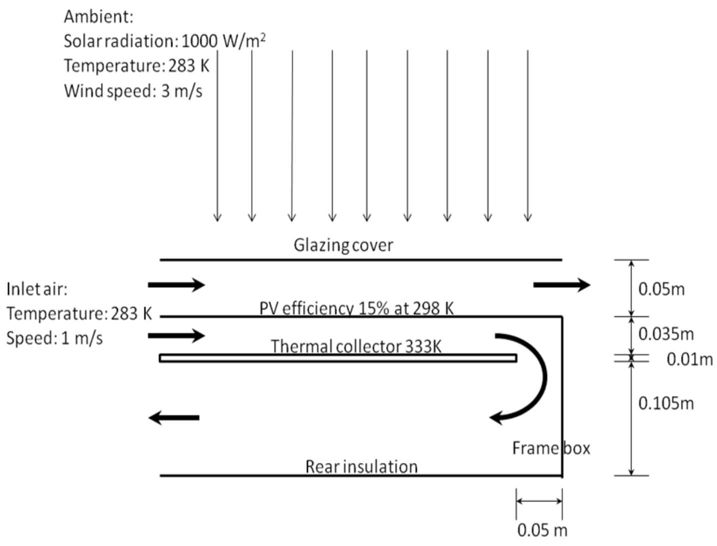

Figure 3: Weather conditions and geometrical parameters of (d) model

3. Mathematical analysis and computer model set-up

In order to use CFD for simulation, two major processes, i.e., solar radiation converted to electricity using PV panel and thermal energy using thermal collector, should be examined. These processes could be illustrated as follows:

3.1 Solar radiation converted to electricity using PV panel

When the solar transmittance of the glazing covers was assumed to be 0.92 for unglazed models and 0.84 for glazed models (Tonui and Tripanagnostopoulos, 2007), the optical and thermal parameters of glazing cover and PV panel were shown in Figure 4.

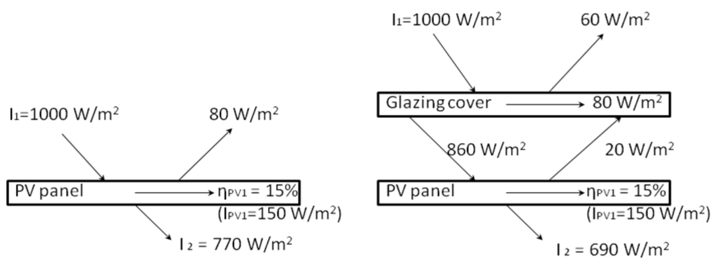

Figure 4: Optical and thermal parameters of glazing cover and PV panel for unglazed and glazed models

Therefore, the solar radiation arriving at the PV panel for the unglazed type and glazed type were 920 and 840 W/m^2, respectively, by deducting the solar radiation absorbed and reflected. The electrical efficiency of PV panel was assumed to 15% at the standard condition with temperature at 15 ^oC and the solar radiation at 1000 W/m^2. Therefore, the solar radiation converted to electricity on PV panel surface would be 150 W/m^2. That left 770 W/m^2 and 690 W/m^2 for the thermal energy generation, respectively.

3.2 Solar radiation converted to heat using thermal collector

One hypothesis of this system was no air leaks as the whole system was perfectly sealed, which meant that there were no energy losses.

Energy can be transferred by three means, conduction, convection and radiation. However, as the thickness of PV panel was small, therefore, the conduction can be omitted.

The convective (W_{con}) and radiative (W_{rad}) heat flux can be expressed as follows, respectively (China Tianjin Chemical Engineering Staff Room, 1983):

$$W_{con} = \frac{t_{PV} - t_{air}}{1/h_{con} A_{PV}} \tag{1}$$

$$W_{rad} = \frac{t_{PV} - t_{air}}{1/h_{rad} A_{PV}} \tag{2}$$

Where t_{PV} (PV panel surface temperature), t_{air} (air temperature) and A_{PV} (PV panel surface area) could be considered as fixed. Therefore, the energy flux had a direct relation to the heat transfer coefficient (h_{con} and h_{rad}), which was illustrated below.

Taking the unglazed PV panel (a) model for example as shown in Figure 5, the convective heat transfer coefficients, h_{con}, could be expressed in Eq. (3), when the air flowing over the PV panel and Eq. (4) when the air flowing in the air passages under the PV panel, according to Taine and Petit (1993).

$$h_{con,PV2} = 5.621 + 3.912 v_{air} \tag{3}$$

$$h_{con,PV3} = 0.029 \mathrm{Pr}^{1/3} \mathrm{Re}^{0.8} \lambda_{PV} / L_{PV} \tag{4}$$

Where v_{air} was the air flow velocity across the PV panel, λ_{PV} was the thermal conductivity of the PV panel and L_{PV} was the length of the PV panel in the air flow direction. Re and Pr were the Reynolds and Prandtl number shown in Eq. (5) and Eq. (6), respectively.

$$\mathrm{Re} = \frac{v_{air} D_{PV} \rho}{\mu} \tag{5}$$

$$Pr = \frac{\mu C_p}{\lambda_{PV}} \quad (6)$$

Where D_{PV} was the hydraulic diameter of the air passages under the PV panel. ρ, μ, C_p were the air flow parameters related to temperature, representing the density, dynamic viscosity, and specific heat capacity.

The radiative heat transfer coefficient, h_{rad}, could be expressed as follow by using the same equation:

$$h_{rad} = \sigma\varepsilon({t_{PV}}^2 + {t_{air}}^2)(t_{PV} + t_{air}) \quad (7)$$

Where σ was the Stefan Boltzman constant at $5.67*10^{-8}$ $W/m^{2}\cdot K^4$ and ε was the emissivity of the PV panel.

Therefore, the heat transfer coefficient could be described as the sum of convective and radiative heat transfer coefficients, which was illustrated below in two different conditions:

$$h_{PV2} = h_{con,PV2} + h_{rad,PV2} \quad (8)$$

$$h_{PV3} = h_{con,PV3} + h_{rad,PV3} \quad (9)$$

So the thermal efficiency under the unglazed PV panel, η_{PV3}, can be expressed as:

$$\eta_{PV3} = \frac{h_{PV3}}{h_{PV2} + h_{PV3}} \quad (10)$$

The solar radiation (I_2) used to generate thermal energy, I_{PV3}, could be expressed in Eq. (11) and illustrated in Table 1:

$$I_{PV3} = \alpha_{PV}\eta_{PV3}I_2 \quad (11)$$

Where α_{PV} was the transparent factor (0.5 for semi-transparent and 1 for opaque).

In this unglazed case, the solar radiation above the PV panel, I_{PV2}, was 0 as the heat was removed by the ambient air flow.

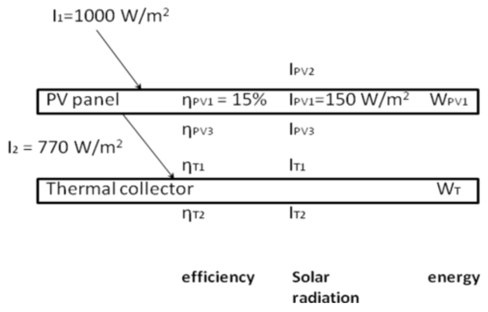

Figure 5: The related parameters of (a) model

According to the equations from (1) to (11), all the solar radiation above and under PV panel (I_{PV2} and I_{PV3}) and above and under thermal collector (I_{T1} and I_{T2}) could also be attained and the results were shown in Table 1 and 2, respectively.

Table 1: Solar radiation above and under PV panel (Units: t (K), D (m), h (W/m^{2}·K), I (W/m^{2}))

	D_{PV2}	Re	$h_{con,PV2}$	$h_{rad,PV2}$	h_{PV2}	D_{PV3}	Re	$h_{con,PV3}$	$h_{rad,PV3}$	h_{PV3}	η_{PV3}	I_{PV2}	I_{PV3}
a	*0*	*0*	*17.36*	*5.01*	*22.4*	*0.035*	*4703*	*16.05*	*5.01*	*21.1*	*0.49*	*0*	*187*
b	*0*	*0*	*17.36*	*5.01*	*22.4*	*0.035*	*4703*	*16.05*	*5.01*	*21.1*	*0.49*	*0*	*187*
c	*0.05*	*6719*	*14.94*	*5.01*	*20.0*	*0.035*	*4703*	*16.05*	*5.01*	*21.1*	*0.52*	*168*	*177*
d	*0.05*	*6719*	*14.94*	*5.01*	*20.0*	*0.035*	*4703*	*16.05*	*5.01*	*21.1*	*0.52*	*168*	*177*
e	*0*	*0*	*17.36*	*5.01*	*22.4*	*0.15*	*20156*	*12.00*	*5.01*	*17.0*	*0.43*	*0*	*333*
f	*0.05*	*6719*	*14.94*	*5.01*	*20.0*	*0.15*	*20156*	*12.00*	*5.01*	*17.0*	*0.46*	*373*	*317*
g	*0.05*	*6719*	*14.94*	*5.01*	*20.0*	*0.15*	*20156*	*12.00*	*5.01*	*17.0*	*0.46*	*373*	*317*

Table 2: Solar radiation above and under thermal collector (Units: t (K), D (m), h (W/m^{2}·K), I (W/m^{2}))

	D_{T1}	Re	$h_{con,T1}$	$h_{rad,T1}$	h_{T1}	D_{T2}	Re	$h_{con,T2}$	$h_{rad,T2}$	h_{T2}	η_{T2}	I_{T1}	I_{T2}
a	*0.035*	*4422*	*15.27*	*6.00*	*21.28*	*0.105*	*13266*	*12.26*	*6.00*	*18.27*	*0.46*	*100*	*86*
b	*0.035*	*4422*	*15.27*	*6.00*	*21.28*	*0.105*	*13266*	*12.26*	*6.00*	*18.27*	*0.46*	*100*	*86*
c	*0.035*	*4422*	*15.27*	*6.00*	*21.28*	*0.105*	*13266*	*12.26*	*6.00*	*18.27*	*0.46*	*95*	*82*
d	*0.035*	*4422*	*15.27*	*6.00*	*21.28*	*0.105*	*13266*	*12.26*	*6.00*	*18.27*	*0.46*	*95*	*82*
e	*0.15*											*333*	
f	*0.15*											*317*	
g	*0.15*											*317*	

3.3 CFD model set-up

Seven computer models were set-up by using CFD program after the predicting calculation of the solar radiation on PV panel and thermal collector. The geometrical parameters, weather conditions and factors relating to air flow, illustrated above, would be input into the CFD program for further simulation.

4. Simulation results and discussions

The simulation results, including the analysis of velocity magnitude, static temperature and static pressure, will be explained below. The key factors judging the performance of the system, electricity generation and thermal energy production, will be discussed further.

4.1 Analysis of velocity magnitude, static temperature and static pressure

Taking (d) model for example, the velocity change of the air flow was shown in Figure 6. The air velocity increased along with the air flowing. As to the constraint of the system structure, turbulence was formed at the corner with the lowest air velocity, which was obvious at the right corner where the air circulating under the thermal collector. After that, the air velocity tended to be maintained at constant.

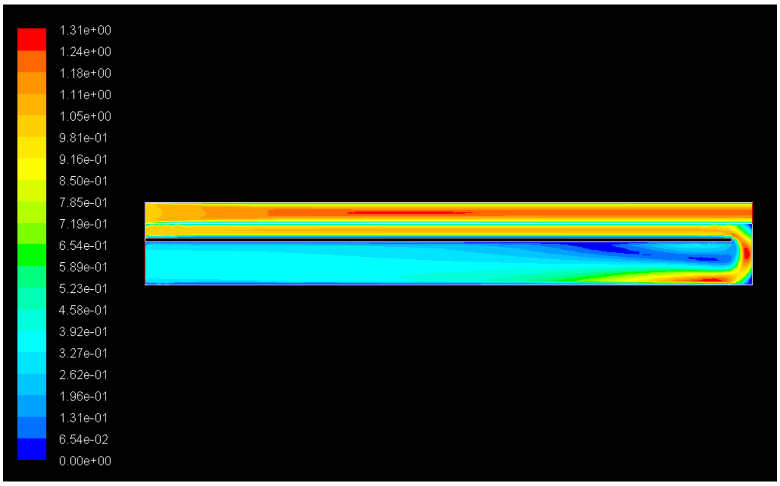

Figure 6: (d) model: image of velocity magnitude

The air temperature increased with the air flowing in the passages, this was because the heat generated by this system was removed by air flow resulting in the air temperature increasing. The air pressure dropped along the air circulating, conversely.

4.2 Analysis of electricity production

The electrical efficiency of PV panel always changed with its temperature. The instantaneous electrical efficiency of PV panel, η_{PV1}, can be expressed as (Godfrey, 2004):

$$\eta_{PV1} = \eta_r (1 - \beta_{PV} (t_{PV} - t_r)) \tag{12}$$

Where η_r and t_r were the reference efficiency and temperature at the standard condition, β_{PV} was the PV panel temperature loss coefficient.

The electricity generated by the PV panel, W_{PV1}, can be expressed as (Wu, 2005):

$$W_{PV1} = \eta_{PV1} I_1 A_{PV} \tag{13}$$

However, in order to maintain the velocity of air flow, part of energy will be consumed by fan (W_f), which can be expressed as (Wu, 2005):

$$W_f = \frac{V_{air} \Delta P}{\eta_f} \tag{14}$$

Where V_{air} was the air volume flow rate, η_f (fan efficiency) was taken as 60% and ΔP was the total pressure drop through the system shown in Eq. (15), including inlet (ΔP_{in}) and outlet (ΔP_{out}) pressure drop caused by air flow velocity and static pressure (ΔP_s) drop from inlet (P_{in}) to outlet (P_{out}), which were expressed at Eqs. (16) and (17).

$$\Delta P = \Delta P_{in} - \Delta P_{out} + \Delta P_s \tag{15}$$

$$\Delta P_{in\,or\,out} = k_{in\,or\,out} \frac{1}{2} \rho v_{air}{}^2 \tag{16}$$

$$\Delta P_s = P_{in} - P_{out} \tag{17}$$

Where $k_{in\ or\ out}$ was the pressure loss coefficient at the inlet and outlet of the system.

The net electricity production, W_{net}, can be described as:

$$W_{net} = W_{PV1} - W_f \tag{18}$$

In this calculation, the average temperature of PV panel and the relevant pressure drops can be attained after simulation as shown in Table 3. The results of net electricity generation were presented in this Table as well.

Table 3: Electricity production

	t_{PV} (K)	η_{PV1}	W_{PV1} (W)	ΔP_{in} (Pa)	ΔP_{out} (Pa)	ΔP_s (Pa)	ΔP (Pa)	W_f (W)	W_{net} (W)
a	*302.135*	*0.1472*	*220.8*	*1.226*	*0.612*	*1.6442*	*2.2582*	*0.56455*	*220.2355*
b	*307.7077*	*0.1434*	*215.1*	*0.613*	*0.306*	*0.905*	*1.212*	*0.0707*	*215.0293*
c	*307.4939*	*0.1436*	*215.4*	*1.839*	*0.918*	*2.4724*	*3.3934*	*1.131133*	*214.2689*
d	*312.741*	*0.1401*	*210.15*	*1.226*	*0.612*	*1.7479*	*2.3619*	*0.334603*	*209.8154*
e	*316.9249*	*0.1372*	*205.8*	*0.613*	*0.306*	*0.2527*	*0.5597*	*0.139925*	*205.6601*
f	*317.0622*	*0.1371*	*205.65*	*1.226*	*0.612*	*1.081*	*1.695*	*0.565*	*205.085*
g	*320.3494*	*0.1349*	*202.35*	*0.613*	*0.306*	*1.4451*	*1.7521*	*0.146008*	*202.204*

From this Table, maintaining two out of three aspects constant and changing only one aspect, the results would be as follows:

For the models with or without glazing covers, it was found that the electricity generation of the unglazed PV panels was higher than the ones with glazing covers. Although the glazing could provide protection for the system, it increased its temperature which minimized the production of electricity eventually.

Comparing the models with semi-transparent or opaque PV panel, it was found that the models with semi-transparent PV panel could generate higher net electricity than the opaque models, this was because the heat generated by PV panel in opaque models were higher than that in semi-transparent models, which increased the system temperature and minimized the capability of PV panel.

About the air flow direction in the models, it was found that the straight flow will eliminate more heat, decrease the temperature of PV panel and maintain a high electricity generation of PV panels than the U-shape air flow models when the air flow velocity constant.

4.3 Analysis of thermal energy production

The thermal energy generated by thermal collector, W_T, could be expressed as follows (Wu, 2005):

$$W_T = \rho V_{air} C_p (t_{out} - t_{in}) \tag{19}$$

The air temperature at the inlet and outlet of the system, t_{in} and t_{out}, were shown in Table 4 with the thermal energy production as well.

Table 4: Thermal energy production

	v *(m/s)*	*V* *(m^3/s)*	t_{in} *(K)*	t_{out} *(K)*	*Heat recovered*	W_T *(W)*
a	*1*	*0.035*	*283.0829*	*293.5174*	*443.5076*	*598.8593*
	1	*0.105*	*283.0181*	*284.2364*	*155.3517*	
b	*1*	*0.035*	*283.0503*	*295.9069*	*546.4578*	*546.4578*
c	*1*	*0.05*	*283.0301*	*293.9231*	*661.4242*	*1233.273*
	1	*0.035*	*310.3664*	*320.3352*	*423.7135*	
	1	*0.105*	*291.8766*	*293.0383*	*148.1358*	
d	*1*	*0.05*	*283.0282*	*293.962*	*663.8985*	*1182.493*
	1	*0.035*	*283.3918*	*295.5929*	*518.5947*	
g	*1*	*0.15*	*283.0336*	*286.5999*	*649.6463*	*649.6463*
h	*1*	*0.05*	*283.0353*	*293.5208*	*636.679*	*1279.624*
	1	*0.15*	*283.0058*	*286.5354*	*642.9446*	
i	*1*	*0.05*	*283.0788*	*302.2632*	*1194.876*	*1194.876*

The variation of thermal energy production with different models can be summarised as follows:

For the comparison of the models with and without glazing, it was found that the one with glazing covers will generate much more thermal energy as to the ability of glazing covers, minimizing the thermal emission, which was thus the key to determine the heat amount.

About the transparency of the PV panel, it was obvious that the opaque models had higher thermal energy generation as the solar radiation was transmitted through the opaque PV panel without the constraint of the materials of PV panel.

About the thermal energy generation with different air flow directions, the straight flow was confirmed as the most efficient way for the heat generation.

5. Conclusion

This paper described seven different models of PV/T collector. CFD program was used to analyse the performance of these models. The major findings could be outlined as below:

For all the seven models, the air velocity raised up gradually as the flow would be enhanced by the structure of the collector. The static temperature increased as the heat generated would be absorbed by the air flow, which would also cause the static pressure decreased along the air flow.

For the models with or without glazing covers, it was found that the unglazed PV panels would generate more electricity than the ones with glazing covers, while less thermal energy. Comparing the models with semi-transparent and opaque PV panel, it was found that the models with semi-transparent PV panel could generate higher net electricity than the opaque models, while produce less thermal energy as well. In terms of the air flow directions in the models, the straight air flow models would generate more electricity and more thermal energy than the U-shape models.

References

Charalambous P G, Maidment G G, Kalogirou S A, Yiakoumetti K (2007) *Photovoltaic Thermal (PV/T) Collectors: A Review*, Applied Thermal Energy **27**: 275-286.

China Tianjin Chemical Engineering Staff Room (1983) *Principles of Chemical Industry,* one ed., Tianjin Science and Technology Press, pp. 213-268.

Godfrey B (2004) *Renewable Energy: Power for a Sustainable Future*, Oxford University Press.

Modest M F (1993) *Radiation Heat Transfer*, New York, McGraw-Hill Inc.

Taine J and Petit J P (1993) *Heat Transfer*, UK, Prentice Hall International.

Tonui J K and Tripanagnostopoulos Y (2007) *Air Cooled PV/T Solar Collectors with Low Cost Performance Improvements,* Solar Energy **81**: 498-511.

Wu Y (2005) *CFD Simulation of the Performance of Photovoltaic-Thermal Collector,* University of Nottingham, Ph.D. Thesis, pp. 23 and 38-41.